Journal of Materials Chemistry C

PAPER

View Article Online
View Journal

Cite this: DOI: 10.1039/c5tc02616d

Photosensitive polystyrene/silver bromide hybrid colloidal crystals as recoverable colorimetric naked eye probes for bromine gas sensing†

Bing Yu,* Feng Zhai, Hailin Cong* and Di Yang

Received 22nd August 2015,
Accepted 8th December 2015

DOI: 10.1039/c5tc02616d

www.rsc.org/MaterialsC

Photosensitive polystyrene (PS)/silver bromide (AgBr) hybrid colloidal crystals were prepared using a co-deposition method. After treatment with UV light, the infiltrated AgBr decomposed to silver nanoparticles (Ag-NPs), and PS/Ag-NP hybrid colloidal crystals with enhanced structural colours were obtained. The enhanced structural colors are due to the absorption of incoherent scattering light and increase in color saturation by the embedded Ag-NPs. The band gaps of the PS colloidal crystals, and PS/AgBr and PS/Ag-NP hybrid colloidal crystals were measured using a UV-vis reflection spectrometer and calculated using Bragg law. The obtained PS/Ag-NP hybrid colloidal crystals could be used as recoverable colorimetric naked eye probes for bromine (Br) gas sensing with a detection limit of 15 mmol L^{-1} at a sensing time of 50 s. The sensor had a very reliable performance after repeated bromine sensing, and could be mass produced facilely with very low cost.

Introduction

Gas sensors can detect combustible, explosive and toxic gases, and are becoming more and more important because they can be widely used in many fields such as industrial emission control, household security, vehicle emission control and environmental monitoring.[1–4] There is also an ever increasing demand for simple and reliable assay methods for industrial gas leakage detection, such as halogen vapours and acidic gases from preparation processes, to face the increasingly serious energy crisis and environmental pollution issues.[5–7] Bromine (Br) gas usually comes from metallurgy, papermaking, pharmaceuticals, pesticides, and chemical and other industries.[8–10] Since bromine gas is highly toxic and has a cumulative effect in living creatures, it is necessary to detect and monitor bromine gas in the environment. At present, the main methods of detecting bromine gas include electrochemical, optical, semiconductor and gas chromatography. Overall, detection equipment is quite expensive and complicated. Thereby, a simple and facile method should be further developed.

Colloidal crystals have been popular due to their intriguing properties and variety of applications in different fields such as sensors, optoelectronic devices, supported catalysis and displays.[11–15] Colloidal crystals consist of nano- or micro-sized silica or polymer microspheres in ordered arrays that are capable of reflecting light at a specific band gap due to the periodic variation of the refractive index in the crystals.[16–18] They have been extensively studied and explored as potential sensors due to the high sensitivity of the band gap to the variations of the lattice spacing and/or refractive index.[19–21] With the appropriate transformation of external conditions, the structural color/band gap of a colloidal crystal alters correspondingly. In view of this characteristic, the tuneable materials operating in the visible region are of special interest, and can be used as important colorimetric materials with wide applications in naked eye sensors.[22–26] Monodisperse colloids usually adopt face centered cubic (fcc) packing in colloidal crystals, leaving a void ratio of ~26% in the structure. The voids were easily infiltrated with guest molecules or nanoparticles through different strategies.[27–30] For example, Cao *et al.* fabricated fluorescent sensor materials by the infiltration of CdTe and CdSe quantum dots into the voids of colloidal crystals using a co-deposition method.[31] Endo *et al.* developed a colloidal crystal-based colorimetric chemical sensor for volatile organic compound (VOC) detection by infiltrating functional polymers into the voids of colloidal crystals.[32]

Silver bromide (AgBr), can be decomposed under UV irradiation to form silver nanoparticles (Ag-NPs) and bromine gas. However, AgBr can be synthesized by putting Ag-NPs and bromine gas together without UV irradiation.[33–36] Therefore, the reversible reactions of AgBr have been used widely in photochromic glasses.[37]

In this paper, photosensitive polystyrene (PS)/AgBr hybrid colloidal crystals were prepared using a co-deposition method. After treatment with UV irradiation, PS/Ag-NP hybrid colloidal

Laboratory for New Fiber Materials and Modern Textile, Growing Base for State Key Laboratory, College of Chemical Engineering, Qingdao University, China. E-mail: yubingqdu@yahoo.com, hailincong@yahoo.com; Fax: +86 532 85955529; Tel: +86 532 85953995

† Electronic supplementary information (ESI) available. See DOI: 10.1039/c5tc02616d

crystals with enhanced structural colours were obtained. The possible reasons for the phenomena were investigated. The application of the PS/Ag-NP hybrid colloidal crystals as recoverable colorimetric probes for bromine gas sensing was studied and discussed preliminarily.

Experimental

Chemicals

Styrene (St, 98%) and methyl methacrylate (MMA, 99.5%) were purchased from Tianjin Wingtai Chemical Company, and were distilled under vacuum before use. 3-Sulfopropyl methacrylate potassium salt (SPMAP, 96%) was purchased from Aladdin Reagent Company. Ammonium persulfate ($(NH_4)_2S_2O_8$, 99.6%) and ammonium bicarbonate (NH_4HCO_3, 21.0–22.0%) were purchased from Tianjin Ruijinte Company. Silver nitrate ($AgNO_3$, 99.9%) was purchased from National Medicine Company. Potassium bromide (KBr, 99%) was purchased from Tianjin Beichen Reagent Company. Polyvinyl pyrrolidone (PVP, 99%) was purchased from Tianjin Fine Chemical Company. Br_2 (99.8%) was purchased from Tianjin Chemical Company. All the chemicals were used as received unless noted elsewhere.

Synthesis of monodisperse PS latex particles

Monodisperse PS latex was synthesized by the emulsion polymerization of St according to a method described elsewhere.[38,39] The average particle diameter of a typical sample is 200 nm with a polydispersity index of less than 3%. The latex was purified using a centrifugal method and dried at 40 °C to obtain the PS particles for further use.

Synthesis of AgBr nanoparticles

The AgBr nanoparticles with an average diameter of ~16 nm were prepared as follows: 0.1 g of PVP, 0.85 g of $AgNO_3$ and 50 mL of deionized water were added into a 150 mL brown conical flask. After stirring at 200 rpm for 30 min at room temperature, 10 mL of KBr aqueous solution with a concentration of 0.5 mol L^{-1} was added into the conical flask within 1 min. After reaction for 4 h under room temperature, the mixture was purified using the centrifugal method and dried at 40 °C to obtain the AgBr nanoparticles for further use.

Preparation of PS/AgBr hybrid colloidal crystals

0.038 g of the PS particles, 0.0075–0.015 g of the AgBr nanoparticles and 4 mL of deionized water were added into a 5 mL weighing bottle. The mixture was dispersed uniformly under ultrasonic conditions at 100 W for 30 min. After co-deposition for 5 days under a dark environment at room temperature, PS/AgBr hybrid colloidal crystals with interspaces filled with AgBr nanoparticles were obtained.

Preparation of PS/Ag-NP hybrid colloidal crystals

The PS/Ag-NP hybrid colloidal crystals were obtained after UV treatment of the PS/AgBr hybrid colloidal crystals for 10 min at an intensity of 620 μw cm^{-2} (365 nm). In this process, the infiltrated AgBr nanoparticles in the colloidal crystals were decomposed *in situ* into Ag-NPs. The obtained PS/Ag-NP hybrid colloidal crystals were put into bromine gas of different concentrations with a digital camera (Nikon D3200) to record the surface color after 50 s.

Characterization

The morphology and size of the obtained colloidal crystals and particles were investigated using scanning electron microscopy (SEM, JEOL JSM-6309LV) and transmission electron microscopy (TEM, JEOL JEM-1200). The optical properties of the colloidal crystals were characterized using a UV-vis reflection spectrometer (Ocean Optics USB-2000) equipped with a 150 W haloid lamp cold light (Lamp-house YN XD-301). The UV-vis spectra were collected under the perpendicular irradiation of cold light. The UV-vis absorbance of all liquid samples was detected with a UV-vis spectrometer (Puxi TU-1810).

Results and discussion

Fig. 1 shows the SEM images of the PS/AgBr hybrid colloidal crystals formed at different AgBr nanoparticle concentrations. Without adding the AgBr nanoparticles (Fig. 1a and c), the colloidal crystal of the 200 nm PS latex particles has voids (black regions) in the structures. After co-deposition with 0.01 mol L^{-1} AgBr nanoparticles (Fig. 1b and d), the voids in the colloid crystal structures are filled very well. Too high concentrations of the AgBr nanoparticles such as 0.015 mol L^{-1} and 0.02 mol L^{-1} lead to overloading and disorder of the formed hybrid colloidal crystals (Fig. 1e and f). Therefore, AgBr nanoparticles with a

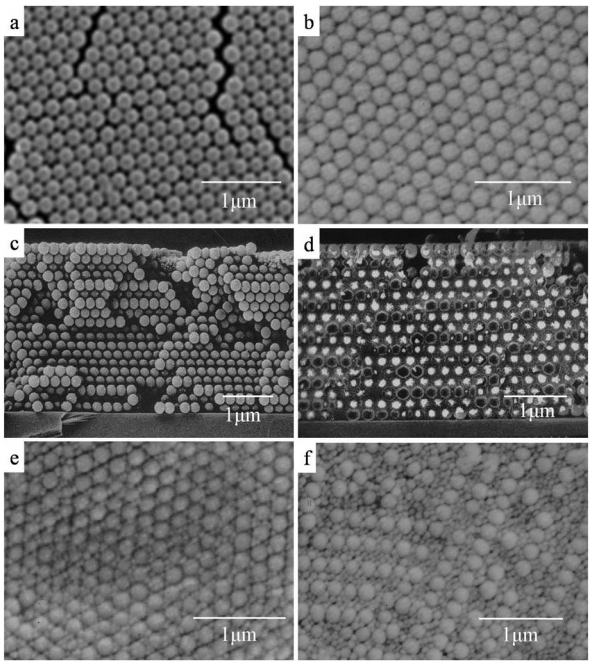

Fig. 1 SEM images of PS/AgBr hybrid colloidal crystals formed at different AgBr nanoparticle concentrations: (a) 0 mol L^{-1}; (b) 0.01 mol L^{-1}; (c) section view of (a); (d) section view of (b); (e) 0.015 mol L^{-1}; (f) 0.02 mol L^{-1}.

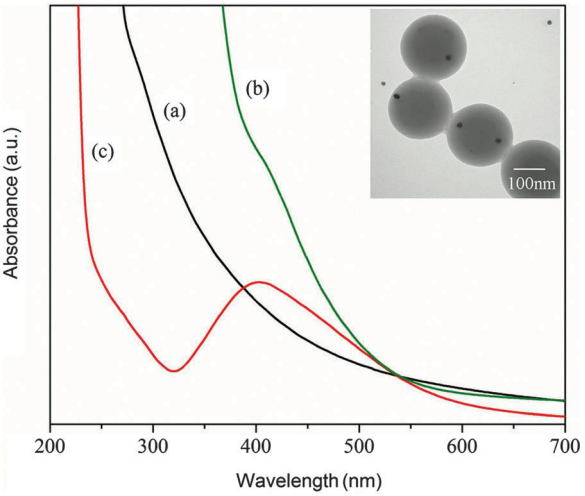

Fig. 2 UV-vis spectra of aqueous dispersions of pure PS colloidal crystals (a), and PS/AgBr (b) and PS/Ag-NP (c) hybrid colloidal crystals. (The inset is a TEM image of the dried PS/Ag-NP hybrid colloidal crystal dispersions.)

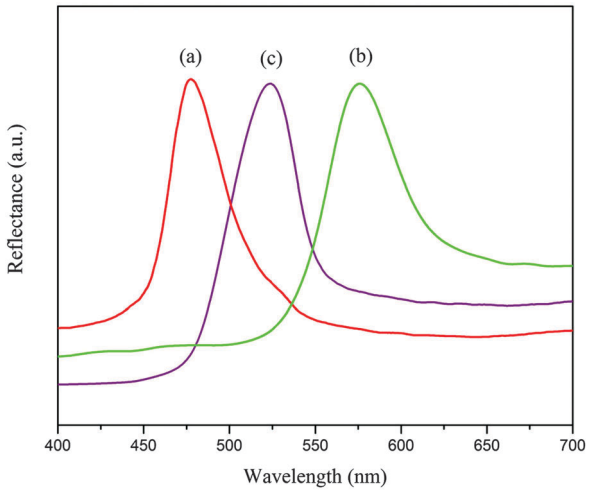

Fig. 3 UV-vis reflection spectra of pure PS colloidal crystals (a), and PS/AgBr (b) and PS/Ag-NP (c) hybrid colloidal crystals. (The spectra are measured at normal incidence.)

concentration of 0.01 mol L^{-1} are selected in our experiments to make the PS/AgBr hybrid colloidal crystals.

Fig. 2 shows the UV-vis spectra of the aqueous dispersions (2 mg mL^{-1}) of the pure PS colloidal crystals, and PS/AgBr and PS/Ag-NP hybrid colloidal crystals. The PS/Ag-NP hybrid colloidal crystals were obtained after UV treatment of the PS/AgBr hybrid colloidal crystals for 10 min at an intensity of 620 μw cm^{-2} and a wavelength of 365 nm. In this process, the infiltrated AgBr nanoparticles in the colloidal crystals were decomposed *in situ* into Ag-NPs. The aqueous dispersions of the PS colloidal crystals, and PS/AgBr and PS/Ag-NP hybrid colloidal crystals were obtained by mixing 0.01 g of the pure PS colloidal crystals, and PS/AgBr and PS/Ag-NP hybrid colloidal crystals in 5 mL of deionized water under ultrasonic dispersion (100 W, 5 min), respectively. By comparing Fig. 2c with Fig. 2a and b, we can see that after the decomposition of AgBr into the Ag-NPs in the hybrid colloidal crystals under UV irradiation, there is a surface plasmon resonance (SPR) peak of the Ag-NPs at 400 nm. As shown in the inset, the TEM image of the dried PS/Ag-NP hybrid colloidal crystal dispersions, the *in situ* generated Ag-NPs (black dots) have an average diameter of ~15 nm.

The maximum band gaps of the colloidal crystals can be calculated according to Bragg's law as shown in eqn (1),[39,40] where λ is the wavelength of the band gap in the (111) direction, k is an arbitrary integer coefficient, D is the diameter of the colloids, n is the refractive index of the colloidal crystal, and θ is the angle of incidence.

$$k\lambda = 2\sqrt{2/3}D\sqrt{n^2 - \sin^2\theta} \quad k = 1, 2, 3, \ldots \qquad (1)$$

In our experiment, incident light is vertical to the (111) surface, so the angle of incidence is zero ($\theta = 0$). The refractive indexes (n) of the PS colloidal crystal, and PS/AgBr and PS/Ag-NP hybrid colloidal crystal can be calculated according to eqn (2),[41] where Φ represents the void ratio of the colloidal crystal (~26%), and n_{ps}, n_{air}, n_{AgBr} and n_{Ag} represent the refractive indices of the PS colloids (~1.59), air (~1.00), AgBr (~2.23) and Ag (~1.67),[42] respectively.

$$n^2 = (1 - \Phi){n_{ps}}^2 + \Phi{n_{air/AgBr/Ag}}^2 \qquad (2)$$

Fig. 3 shows the UV-vis reflection spectra of the structural colors in the pure PS colloidal crystals, and PS/AgBr and PS/Ag-NP hybrid colloidal crystals measured at the normal incidence. The experimental data was detected using an optical fiber spectrometer and the intensity of the reflection was processed in an arbitrary manner to level the height of the peaks. The band gap of the pure PS colloidal crystals is at 475 nm (Fig. 3a), which is very close to the calculated values (476.9 nm) according to eqn (1) and (2). After the incorporation of the AgBr nanoparticles, the band gap shifts to 577 nm (Fig. 3b), which is very close to the calculated values (581.4 nm) according to eqn (1) and (2). After the decomposition of AgBr into the Ag-NPs under UV irradiation, the band gap shifts to 522 nm (Fig. 3c), which is very close to the calculated values (525.5 nm) according to eqn (1) and (2).

Fig. 4a shows the UV-vis reflection spectra of the PS/AgBr hybrid colloidal crystal under different UV irradiation times at an intensity of 620 μw cm^{-2} and a wavelength of 365 nm. The experimental data was detected using the optical fiber spectrometer and the intensity of the reflection was processed in an arbitrary manner to level the height of the peaks. An obvious blue shift of the wavelength can be seen as the time of UV irradiation increases, because the infiltrated AgBr nanoparticles in the colloidal crystals were decomposed *in situ* into the Ag-NPs gradually in this process and caused a gradual decrease of the refractive indices of the hybrid colloidal crystals. There's a linear relationship between the wavelength shift and UV irradiation time (Fig. 4b). After UV irradiation for 10 min, the spectrum of the PS/AgBr hybrid colloidal crystal is no longer changed, which indicates that the infiltrated AgBr is fully decomposed and converted into Ag-NPs.

Fig. 5 shows the photos of the PS colloidal crystals before and after AgBr conversion to Ag-NPs. The pure PS colloidal

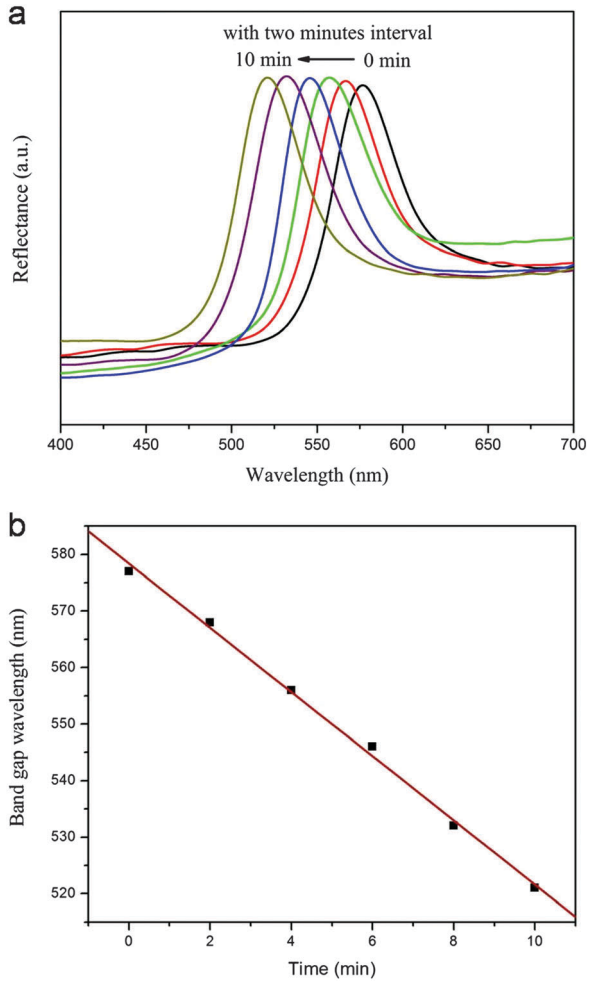

Fig. 4 UV-vis reflection spectra (a), and relationship between the band gap shift and time (b) of the PS/AgBr hybrid colloidal crystal under different UV irradiation times. (The spectra are measured at normal incidence.)

crystal is milky white with a very faint structural color (Fig. 5a). By introducing the Ag-NPs into the lattice structure, the visual appearance of the colloidal crystal changes quite remarkably from milky white to an intense deep green (Fig. 5b). These pictures are taken under natural lighting conditions and show that the color mechanism which should originate from the addition of the Ag-NPs decreases the incoherent scattering light intensity (ESI,† Fig. S1). This phenomenon shows that

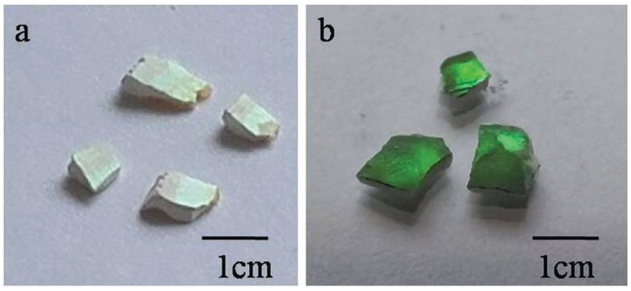

Fig. 5 Photographs of pure PS colloidal crystals (a) and PS/Ag-NP hybrid colloidal crystals (b) at a view angle of 45°.

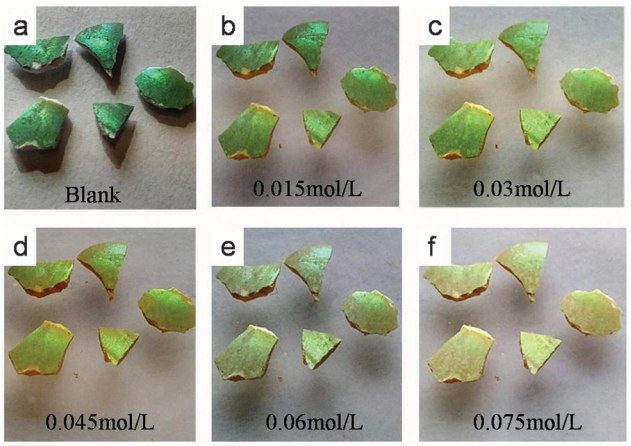

Fig. 6 Photographs of the PS/Ag-NP hybrid colloidal crystal sensor in contact with bromine gas of different concentrations for 50 s: (a) 0 mmol L^{-1}; (b) 15 mmol L^{-1}; (c) 30 mmol L^{-1}; (d) 45 mmol L^{-1}; (e) 60 mmol L^{-1}; (f) 75 mmol L^{-1}.

the Ag-NPs have similar properties to carbon black as reported elsewhere.[43–45] As a consequence, the Ag-NPs may also play a

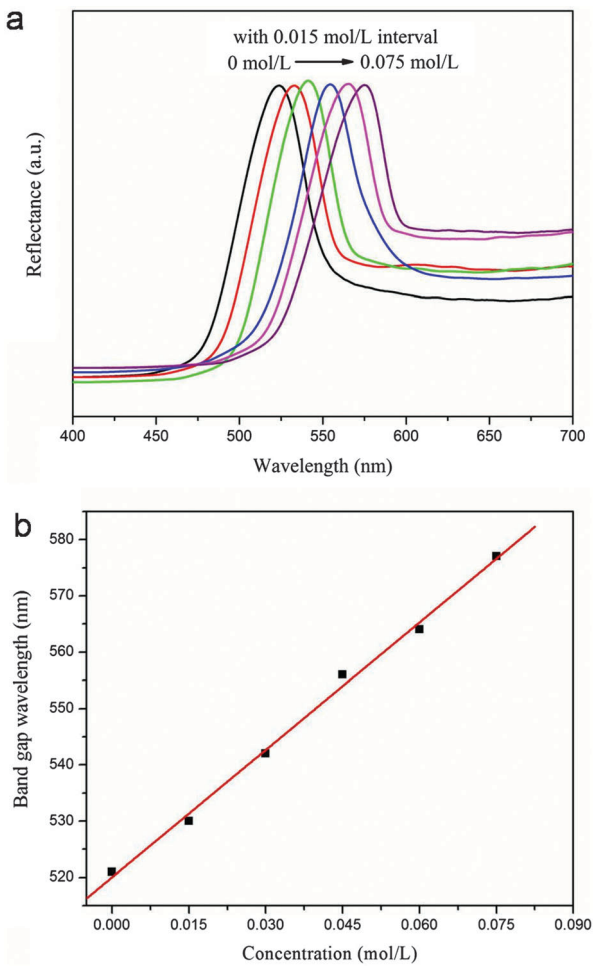

Fig. 7 UV-vis reflection spectra (a) and relationship between the band gap shift and concentration (b) of the PS/Ag-NP hybrid colloidal crystal sensor in contact with bromine gas of different concentrations for 50 s. (The spectra are measured at normal incidence.)

role in absorbing the scattering light and increasing color saturation, which makes the structural color of the colloidal crystals brighter intuitively.

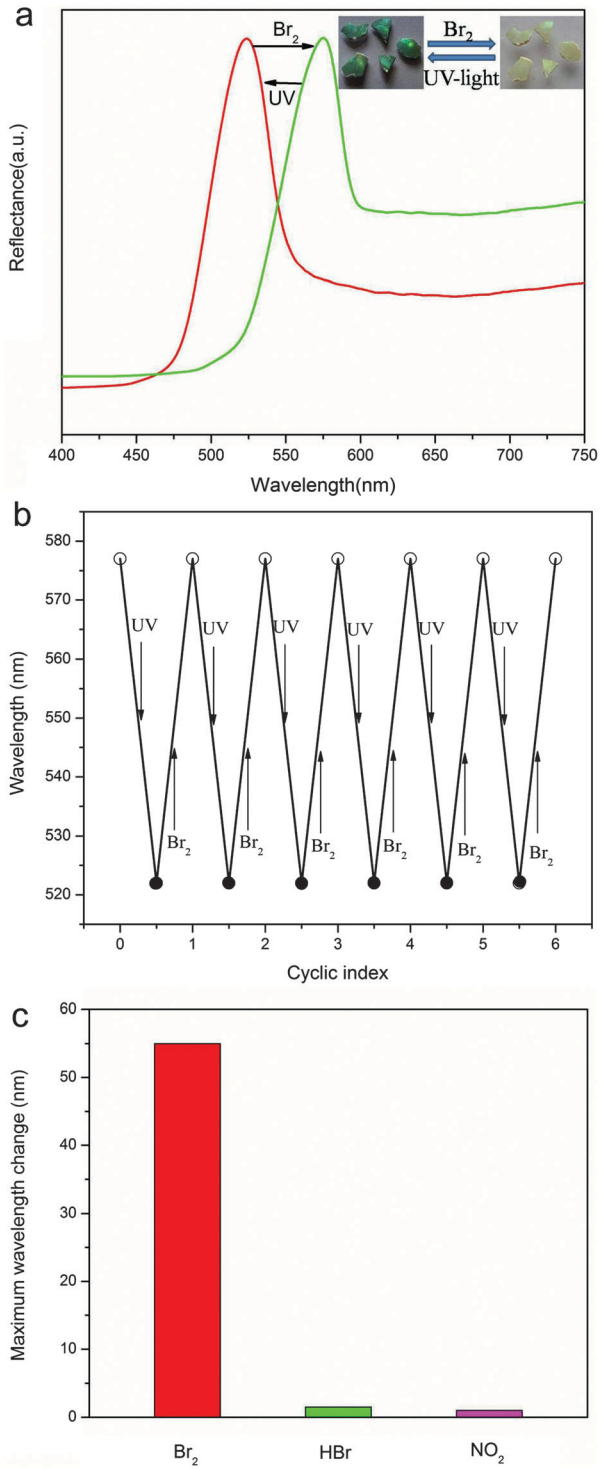

Fig. 8 Regeneration properties of the PS/Ag-NP hybrid colloidal crystal sensor: (a) reflection spectra of bromine gas sensing and the regeneration process, the corresponding photographs are shown in the insets; (b) wavelength position changes of the sensors during six cycles of bromine gas sensing and regeneration; (c) maximum wavelength change of the sensor in contact with 0.075 mol L^{-1} Br_2, HBr and NO_2 gases.

Fig. 6 shows the structural color variation of the PS/Ag-NP hybrid colloidal crystal sensor in contact with bromine gas of different concentrations for 50 s at a view angle of 45°. The sensor itself showed an intense deep green color. After exposure to bromine gas of different concentrations for 50 s, the color changed from a deep green to a light yellow with increased bromine gas concentrations, and the enhanced structural color from the Ag-NPs gradually disappeared.

Fig. 7a shows the UV-vis reflection spectra of the PS/Ag-NP hybrid colloidal crystal sensor on contact with bromine gas of different concentrations for 50 s. The experimental data was detected using the optical fiber spectrometer and the intensity of the reflection was processed in an arbitrary manner to level the height of the peaks. An obvious red shift of the wavelength can be seen as the concentration of bromine gas increases. There's a linear relationship between the wavelength shift and bromine gas concentration (Fig. 7b). After contact with 75 mmol L^{-1} bromine gas for 50 s, the spectrum of the PS/Ag-NP hybrid colloidal crystal sensor is no longer changed, which indicates that the infiltrated Ag-NPs have fully reacted with bromine gas and converted into AgBr.

The reflection spectra of bromine gas sensing and regeneration are shown in Fig. 8a, and the inset photographs are the PS/Ag-NP hybrid colloidal crystal sensor after UV irradiation for 10 min at an intensity of 620 μw cm^{-2} and a wavelength of 365 nm, the PS/Ag-NP hybrid colloidal crystal sensors can be regenerated from the already used sensors. The wavelength data from six cycles of bromine gas sensing and regeneration under UV irradiation is shown in Fig. 8b, and the reflection spectra are shown in the ESI,† Fig. S2. There's no obvious change in the wavelength position of the sensors, which indicates that the PS/Ag-NP hybrid colloidal crystal sensor has a very reliable performance, and can be used as a recoverable colorimetric naked eye probe for bromine gas sensing. In order to further exploit the selectivity of the sensor, interfering gases of HBr and NO_2 are checked with the sensor. As shown in Fig. 8c, the sensor only shows high selectivity and sensitivity to Br_2 gas as compared with the interfering gases.

Conclusions

In this work, photosensitive PS/AgBr hybrid colloidal crystals were prepared successfully by the co-deposition of monodisperse PS latex particles and AgBr nanoparticles. After treatment with UV light, the infiltrated AgBr nanoparticles decomposed to Ag-NPs, and PS/Ag-NP hybrid colloidal crystals with enhanced structural colors were obtained successfully. The measured band gaps of the colloidal crystals were in accordance with the theoretical calculation very well. The enhanced structural colors are due to the decrease of incoherent light scattering and increase of color saturation. The PS/Ag-NP hybrid colloidal crystals could be used as recoverable colorimetric naked eye probes for bromine gas sensing with a detection limit of 15 mmol L^{-1} at a sensing time of 50 s. The sensor has a very reliable performance after repeated bromine gas sensing and regeneration, and could be mass produced facilely with very low cost.

Acknowledgements

This work is financially supported by the National Key Basic Research Development Program of China (973 special preliminary study plan, 2012CB722705), the Natural Science Foundation of China (21375069, 21404065, 21574072), the Natural Science Foundation for Distinguished Young Scientists of Shandong Province (JQ201403), the Project of Shandong Province Higher Educational Science and Technology Program (J15LC20), the Graduate Education Innovation Project of Shandong Province (SDYY14028), the Scientific Research Foundation for the Returned Overseas Chinese Scholars of State Education Ministry (20111568), the Science and Technology Program of Qingdao (1314159jch), the China Postdoctoral Science Foundation (2014M561886, 2015T80695) and the Doctoral Scientific Research Foundation of Qingdao.

Notes and references

1 F. L. Meng, Z. Guo and X. J. Huang, *Trends Anal. Chem.*, 2015, **68**, 37.
2 T. Waitz, T. Wagner, T. Sauerwald, C. D. Kohl and M. Tiemann, *Adv. Funct. Mater.*, 2009, **19**, 653.
3 C. Bartual, A. Akou, C. Thibault, C. Vieu, L. Salmon and A. Bousseksou, *J. Mater. Chem. C*, 2015, **3**, 1277.
4 X. Yu, N. Zhou, S. Han, H. Han, D. Buchholzn and J. Yu, *J. Mater. Chem. C*, 2013, **1**, 6532.
5 N. Zhang, K. Yu, Q. Li, Z. Q. Zhu and Q. J. Wan, *J. Appl. Phys.*, 2008, **103**, 104305.
6 Z. Meng, A. Fujii, T. Hashishin, N. Wada, T. Sanada and J. Tamaki, *J. Mater. Chem. C*, 2015, **3**, 1134.
7 I. Jimenez, J. Arbiol, G. Dezanneau, A. Cornet and J. R. Morante, *Sens. Actuators, B*, 2003, **93**, 475.
8 R. Harrison and J. Webb, *Adv. Agron.*, 2001, **73**, 65.
9 S. Abdul, S. Alawi and A. Zawahry, *Environ. Model. Software*, 2002, **17**, 563.
10 P. M. Lemieux, C. C. Lutes and D. A. Santoianni, *Prog. Energy Combust. Sci.*, 2004, **30**, 1.
11 Y. Li, G. T. Duan, G. Q. Liu and W. Q. Cai, *Chem. Soc. Rev.*, 2013, **42**, 3614.
12 H. Cong, B. Yu, J. Tang, Z. Li and X. Liu, *Chem. Soc. Rev.*, 2013, **42**, 7774.
13 I. Butnar and M. Llop, *Ecol. Econ.*, 2007, **61**, 388.
14 S. Foulger, P. Jiang, Y. Ying, A. Lattam, D. Smith and J. Ballato, *Adv. Mater.*, 2001, **13**, 1898.
15 A. Mihi, C. Zhang and P. Braun, *Angew. Chem., Int. Ed.*, 2011, **50**, 5712.
16 J. P. Ge and Y. D. Yin, *J. Mater. Chem.*, 2008, **18**, 5041.
17 J. H. Holtz and S. A. Asher, *Nature*, 1997, **389**, 829.
18 J. Y. Wang, Y. Cao, Y. Feng, F. Yin and J. P. Gao, *Adv. Mater.*, 2007, **19**, 3865.
19 S. Song, S. Shen, X. Cui, D. Yao and D. Hu, *React. Funct. Polym.*, 2011, **71**, 512.
20 Y. N. Xia, *Adv. Mater.*, 2001, **13**, 369.
21 G. Lu, O. K. Farha and L. E. Kreno, *Adv. Mater.*, 2011, **23**, 4449.
22 D. D. Men, H. H. Zhang, L. F. Huang, D. L. Liu, X. Y. Li, W. P. Cai, Q. H. Xiong and Y. Li, *J. Mater. Chem. C*, 2015, **3**, 3659.
23 W. L. Vos, R. Sprik, A. Blaaderen, A. Imhof, A. Lagendijk and G. H. Wegdam, *Phys. Rev. B: Condens. Matter Mater. Phys.*, 1996, **53**, 16231.
24 S. A. Asher, J. Holtz, L. Liu and Z. J. Wu, *J. Am. Chem. Soc.*, 1994, **116**, 4997.
25 C. I. Aguirre, E. Reguera and A. Stein, *Adv. Funct. Mater.*, 2010, **20**, 2565.
26 L. He, M. Wang and J. Ge, *Acc. Chem. Res.*, 2012, **45**, 1431.
27 J. J. Wang, S. Ahl, Q. Li, M. Kreiter, T. Neumann, K. Burkert, W. Knoll and U. Jonas, *J. Mater. Chem.*, 2008, **18**, 981.
28 F. Li, Y. Qian and A. Stein, *Chem. Mater.*, 2010, **22**, 3226.
29 Z. Z. Gu, A. Fujishima and O. Sato, *Chem. Mater.*, 2002, **14**, 760.
30 H. Cong and B. Yu, *J. Colloid Interface Sci.*, 2011, **353**, 131.
31 L. Yang, Z. Yang and W. Cao, *J. Phys. Chem. B*, 2005, **109**, 11501.
32 T. Endo, Y. Yanagida and T. Hatsuzawa, *Sens. Actuators, B*, 2007, **125**, 589.
33 J. J. Li, Y. Xie, Y. Zhong and Y. Hu, *J. Mater. Chem. A*, 2015, **3**, 5474.
34 G. Tian, Y. Chen, H. L. Bao and H. J. Hu, *J. Mater. Chem.*, 2012, **22**, 2081.
35 C. H. An, J. Z. Wang and C. Qin, *J. Mater. Chem.*, 2012, **22**, 13153.
36 K. B. Li, C. X. Dong, Y. H. Zhang and H. Wei, *J. Mol. Catal. A: Chem.*, 2014, **394**, 105.
37 E. A. Saad, F. H. ElBatal and A. M. Fayad, *Silicon Chem.*, 2011, **3**, 85.
38 H. Cong and W. Cao, *J. Phys. Chem. B*, 2005, **109**, 1695.
39 H. Cong, B. Yu and X. S. Zhao, *Opt. Express*, 2011, **19**, 12799.
40 C. I. Aguirre, E. Reguera and A. Stein, *Adv. Funct. Mater.*, 2010, **20**, 2565.
41 H. Cong and W. Cao, *Langmuir*, 2004, **20**, 8049.
42 P. Winsemius, F. F. Kampen, H. P. Lengkeek and C. G. Went, *J. Phys. F: Met. Phys.*, 1976, **6**, 1583.
43 C. I. Aguirre, E. Reguera and A. Stein, *ACS Appl. Mater. Interfaces*, 2010, **2**, 3257.
44 Y. Takeoka, S. Yoshioka, A. Takano, S. Arai, K. Nueangnoraj, H. Nishihara, M. Teshima, Y. Ohtsuka and T. Seki, *Angew. Chem., Int. Ed.*, 2013, **52**, 7261.
45 S. F. Liew, J. Forster, H. Noh, C. F. Schreck, V. Saranathan, X. Lu, L. Yang, R. O. Prum, C. S. O'Hern, E. R. Dufresne and H. Cao, *Opt. Express*, 2011, **19**, 8208.

